THE DISPATCH

Volume 3, Issue 4 | Defense Threat Reduction Information Analysis Center | *ÁÎÕÁÒÙ 201τ

This Issue

Contact Us

dtriac@dtra.mil
or visit us at
www.dtriac.dtra.mil

From the Program Manager

Welcome to the latest issue of *The Dispatch*. This is the first of two issues that features articles from the Nuclear Technologies personnel, describing some studies and efforts related to high-altitude nuclear effects (HANE) phenomenology. DTRA has a long history in the HANE field and DTRIAC maintains a number of historical records in this area.

This quarter we will introduce you to HANE phenomenology and DTRA's involvement in studying HANE effects. Next quarter's issue will highlight the Large Plasma Device (LAPD) at UCLA as well as other research related to DTRA's work. There are still unanswered questions, and the Nuclear Technologies personnel are on the cutting edge of these studies.

Please contact us directly if you ever have any questions or comments related to DTRIAC at dtriac@dtra.mil.

Thanks,

Joyce Rowell
DTRIAC Program Manager

Introduction

by Maj Julio Villafuerte (DTRA) and Keith Sibert (ARA)

High-altitude nuclear explosions create disturbed atmospheric, ionospheric, and space environments that have effects on military systems operating within or through them. The acronym "HANE" is somewhat ambiguous and can alternately stand for high-altitude nuclear explosions, environments, or effects. DTRA has a long history supporting development of modeling tools for high altitude nuclear environments prediction and system effects. Most recently under the HANEMS program (High-Altitude Nuclear Effects Modeling and Simulation Upgrades), Applied Research Associates (ARA) is addressing modeling gaps in the current set of HANE modeling tools by upgrading existing tools and developing new tools where the existing capability is insufficient. HANE phenomenology spans a large spectrum of physical processes with consequences for a variety of military systems. The following set of articles discusses a subset of HANE phenomenology and effects being addressed under the HANEMS program. Three of the articles cover structured ionization and its effects on radio frequency (RF) systems, artificial radiation belts and their effects on satellites, and late-time electromagnetic pulse and its effects on power grids. Another article suggests ways in which data from the natural space environment can aid in HANE model improvement and validation.

Modeling HANE Impacts on RF Propagation with GSCENARIO and PRPSIM

by Paul Edwardson and Carl Lauer (ARA)

HANE Effects on RF Propagation

The term high-altitude nuclear explosion (HANE) typically refers to a burst at or above the "top" of the atmosphere, which is at roughly 100 km altitude. However, a large yield burst at lower altitude can also exhibit HANE behavior as it will be characterized later. A HANE creates a large number of free electrons that can degrade performance of radio frequency (RF) systems including radar, satellite communications, and the global positioning system. It is convenient to divide HANE impacts on RF system performance into three categories: RF noise, mean path effects, and scintillation of the signal. The ways a HANE might cause physical damage to a system are not discussed here.

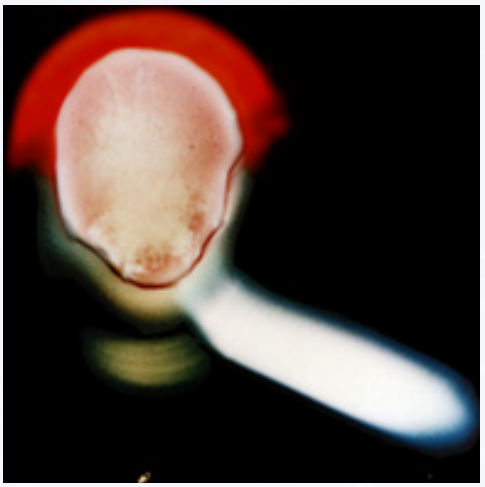

Figure 1. Composite photograph of the KINGFISH fireball and beta patch.

RF noise is generated primarily by random thermal motions of hot electrons, which are abundant in a HANE fireball (Figure 1). The impact of enhanced noise on signal-to-noise ratio depends on the receiving antenna orientation and its field of view relative to the fireball or other hot plasma regions (ions and free electrons).

Mean path effects arise from broad enhancement of the free electron population. Mean effects include absorption of signal power as a radio wave couples to burst-generated electrons, which in turn collide with heavy ions, atoms and molecules, transferring energy from the signal to the environment. Absorption will affect a signal that must pass through the early dense fireball or through radiation-produced ionization lower in the atmosphere. Other mean effects, such as phase shift, delay, and refraction arise from broad enhancement of the index of refraction and its gradient.

RF Scintillation is self-interference of a coherently transmitted signal to produce a received signal that is a convolution of incoherent signals arriving via multiple paths. Scintillation effects are many, including fluctuations in amplitude, phase, arrival time and angle. Scintillation results from variations in the index of refraction associated with small-scale structure in the distribution of free electrons between transmitting and receiving antennae. Scintillation occurs most notably after fireball plasma evolves into long geomagnetic field-aligned striations, and can persist for hours (Figure 2).

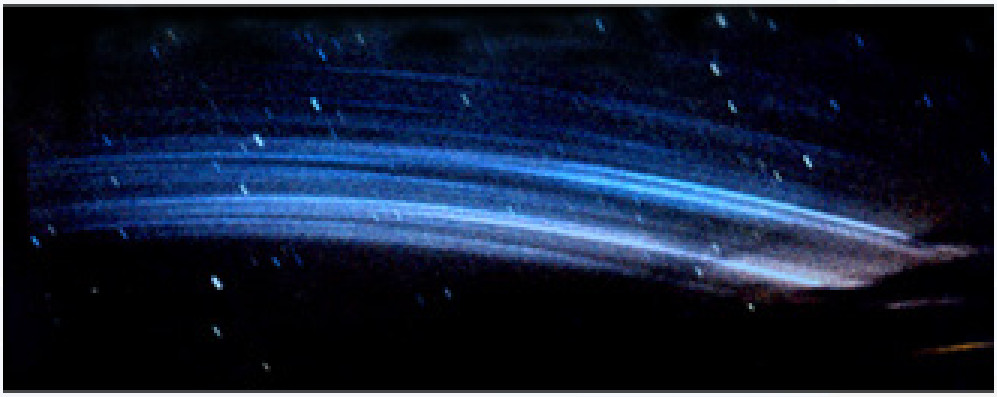

Figure 2. Time-lapse photograph of Checkmate geomagnetic field-aligned plasma striations.

Modeling HANE Impacts on RF Propagation with GSCENARIO and PRPSIM *(continued)*

HANE Phenomenology

After a HANE, energy that will ionize air to free electrons comes in two forms: debris kinetic energy and energetic radiation. Kinetic energy and radiation, respectively, create their most intense ionization above and below the top of the atmosphere.

X and gamma radiation emitted promptly by the burst create broad ionization patches in separate atmospheric regions below the burst. Free electrons recombine quickly in the lower atmosphere, so RF absorption in the prompt x and gamma patches occurs most significantly in the first few tens of seconds after a burst. However, ongoing radioactive decay of weapon debris is a persistent source of atmospheric ionization from both gamma and beta rays.

Beta rays are highly energetic electrons which stream along the geomagnetic field in both directions away from HANE debris. Some emitted beta particles are trapped in the geomagnetic field to form artificial radiation belts (ARB), and others escape into the atmosphere where their energy is absorbed to sustain relatively focused ionization patches. Beta patches can absorb signal power for an extended period. Beta patches can also cause scintillation because their structure reflects the small-scale structure in the high-altitude beta source.

Above the atmosphere, HANE debris kinetic energy is the primary ionization producer. For burst altitudes up to a few hundred kilometers, expanding debris and swept-up air form a blast wave that radiates in the ultraviolet (UV). Re-absorption of radiated UV ahead of the blast wave creates an ionized volume called a UV fireball.

At higher burst altitudes, where air is too thin to support production of a UV fireball, expanding debris ions interact with the geomagnetic field, energizing ambient ions and ions previously produced by x-rays. Those energized ions, along with some debris, stream in both directions along the geomagnetic field to deposit their energy in conjugate kinetic energy patches (KEP) where the geomagnetic field descends into the atmosphere.

A given HANE will exhibit some combination of UV fireball and KEP phenomena in portions depending primarily on burst altitude. No tests were ever conducted with burst altitudes above the KEP regime, but simulation predicts broad weak kinetic energy patches can be created by geomagnetic containment of expanding weapon debris.

KEP regions and UV fireballs are hot and highly ionized. As they rise and expand, recombination chemistry, which consumes free electrons, slows to near insignificance. Perhaps the defining characteristic of a HANE is that after sufficient expansion and cooling, fireball evolution will become governed by the geomagnetic field. The rising HANE fireball or KEP elongates along the geomagnetic field and can eventually stretch over the magnetic equator from one conjugate region to the other.

During transition from rising fireball to magnetic alignment, plasma instabilities can break up burst plasma into narrow field-aligned striations. HANE plasma eventually falls down the geomagnetic field to be consumed by recombination chemistry in the upper atmosphere. This decay of the plasma plume through chemistry at its base can require several hours depending on burst location and yield.

Effects such as RF noise and signal absorption are strongest while HANE generated plasma is dense and hot and while radiation is intense, thus noise and absorption may not seriously impact a given RF system at late times after the burst. Scintillation on the other hand may impact system performance for hours after a HANE.

HANE Modeling for RF Applications

DTRA has developed GSCENARIO and PRPSIM for performance analysis of RF systems operating through HANE environments. GSCENARIO provides HANE environments through which PRPSIM models RF signal propagation, antenna effects, and modem performance. The G in GSCENARIO stands for global, but SCENARIO is not an acronym. GSCENARIO simulations can include any number and arrangement of bursts around the globe, with the current restriction that burst altitudes are in or above the upper atmosphere.

Modeling HANE Impacts on RF Propagation with GSCENARIO and PRPSIM *(continued)*

GSCENARIO models weapon mass and kinetic energy deposition using models developed from outputs of DTRA legacy first-principles codes. GSCENARIO also models x and beta deposition, but not gamma deposition at this time. GSCENARIO evolves the post-deposition environment with chemically reactive magnetohydrodynamics (MHD) of separate but interacting neutral, ion, and electron fluids (Figure 3). Reactive MHD governs evolution of the environment through coupled chemistry and laws of mass conservation, Newton in fluid form, Ampere, and Faraday.

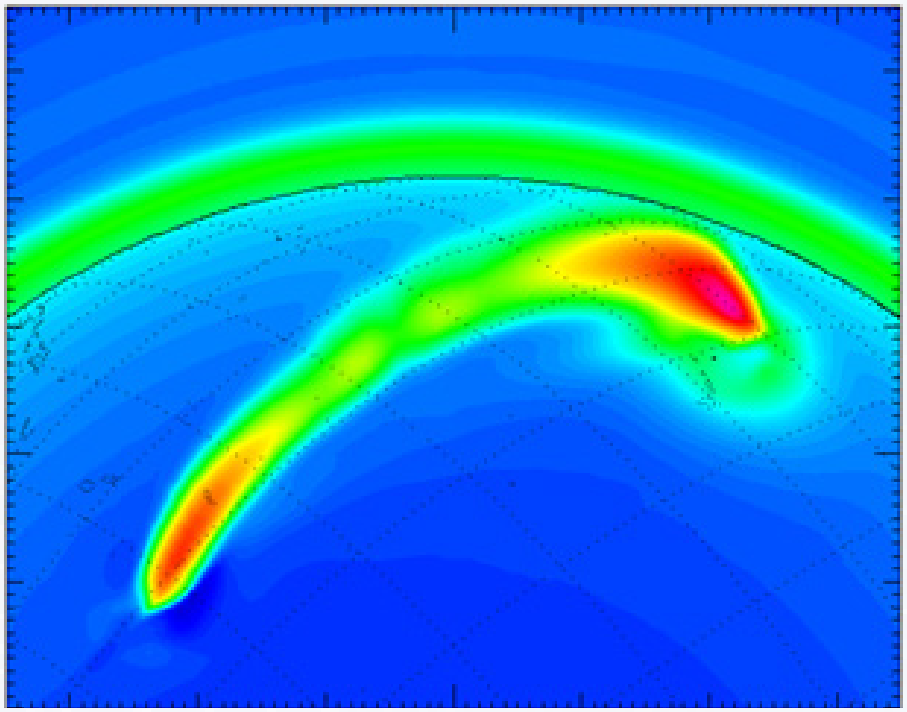

Figure 3. Contours of integrated electron density (known as total electron content or TEC) 5 minutes into a GSCENARIO simulation of a HANE over Honolulu. A combined UV and KEP fireball (red on the right) has risen above the burst region and is stretching along the geomagnetic field to merge with plasma rising from the magnetic conjugate KEP region (red on the left). The blue outside the burst-affected region and green ring around the globe are ambient ionospheric electrons.

GSCENARIO MHD facilitated recent addition of support for ARB simulation, and will facilitate future development of new applications such as infrared environments, and electromagnetic pulse prediction. GSCENARIO MHD also facilitates replacement of legacy code-based and phenomenological models with physics models to improve confidence in predictions. For example, time-of-flight effects were recently added to the KEP deposition model. We also recently began development of a replacement for the legacy phenomenological description of striation statistics shared by GSCENARIO and PRPSIM. Because of their small scale and quasi-random origins, striations and their effects on mean plasma behavior are modeled statistically. The new physics model based on ensemble averages of the MHD equations will replace the phenomenological model and add essential missing elements.

RF Propagation Modeling

The name PRPSIM is an acronym: Properties of Radio Wave Propagation in a Structured Ionized Medium. PRPSIM models RF propagation through the GSCENARIO ambient or disturbed environment using a variant of the multi-phase-screen approach. PRPSIM-computed channel parameters can serve as input to radar and other simulations, or can be used directly within PRPSIM for communication link performance analysis. Channel parameters are combined with PRPSIM antenna filtering and modulation algorithms to determine link budget, margin, signal to noise ratio, bit error rate, and other performance measures.

PRPSIM has been used to simulate complex communication networks. The PRPSIM user can define and orient multiple antennae on platforms with a variety of trajectories. Antennae are paired into links with several waveform and modem design options.

Although PRPSIM can model many systems with high fidelity, PRPSIM modeling is not sufficient to support analyses of all aspects of evolving communication technology or electronic warfare (EW). Future PRPSIM development could support new antennae, waveforms, and EW modeling.

Artificial Radiation Belts

by Keith Siebert and Jay Kerwin (ARA)

A radiation belt is a torus of energetic electrons or protons that encircles the Earth. Naturally occurring radiation belts, the so-called Van Allen belts, were discovered in 1958, and are most often characterized as two tori, an inner belt and an outer belt, separated by a gap called the slot region. In August of last year twin NASA spacecraft, the Van Allen Probes Mission, were launched with instruments to measure radiation belt properties. In February of this year mission researchers announced the discovery of a third, transient belt between the inner and outer belts (Baker, et al. 2013). This belt consisted of highly relativistic electrons of energies from 2 to 6 MeV, and lasted for over four weeks. The creation of a distinct, intense, energetic, and transient belt superposed on the ambient background is reminiscent of a man-made mechanism with similar consequences: a high-altitude nuclear detonation.

After detonation, ionized weapon debris consisting of fission products disperse at high velocity from the burst point. These fission products are radioactive and unstable to beta decay. As a rule of thumb, each fission results in the eventual emission of about six beta electrons. After a beta electron is emitted, it executes three types of periodic motion: gyration around magnetic field lines, bounce motion back and forth along magnetic field lines, and drift motion perpendicular to magnetic field lines and around the Earth. These motions are illustrated in Figure 1. In this way beta electrons are trapped in Earth's magnetic field, creating an artificial radiation belt.

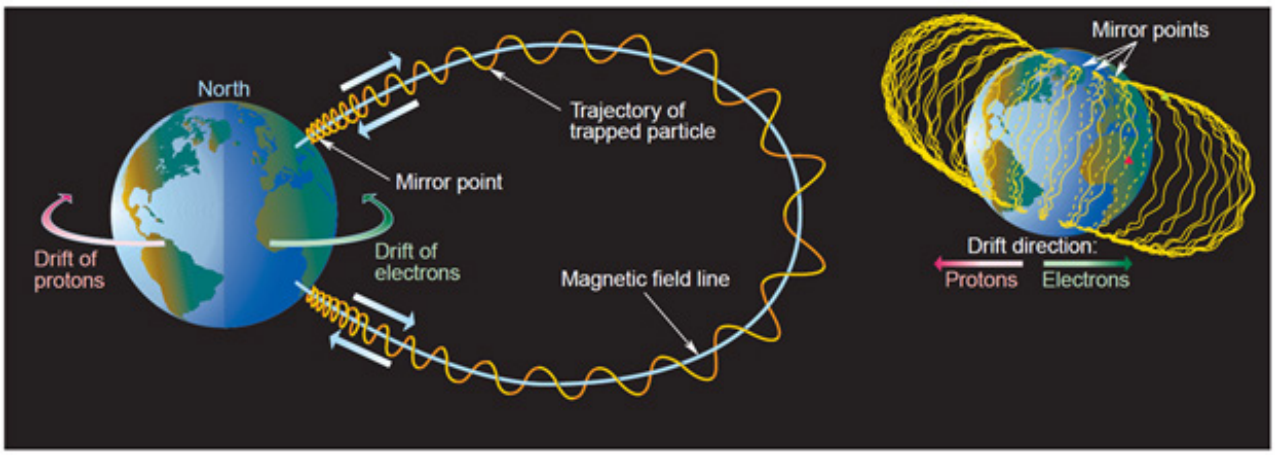

Figure 1. Particle drifts in Earth's magnetic field (from Mazur, 2003)

Probably the best example of an artificial radiation belt was created by the Starfish nuclear test on July 9, 1962. Starfish was a 1.4 MT explosion at 400 km altitude over Johnston Island in the Pacific Ocean. In addition to injection of an artificial radiation belt, Starfish produced a large variety of ionospheric effects including: a diamagnetic cavity or "magnetic bubble" formed by expanding weapon debris (Dyal, 2006), artificial aurora from energized ions streaming along magnetic field lines and colliding with lower-altitude atmospheres in northern and southern conjugate regions, and ionospheric currents that generated late time electromagnetic pulse on the ground. While the creation of an artificial radiation belt by the Starfish explosion was anticipated, its spatial extent was not. A useful coordinate for characterizing the spatial distribution of radiation belts is the McIlwain L parameter (McIlwain, 1961). The L value of a magnetic field line in a dipole magnetic field specifies the distance measured in Earth radii from the center of the Earth to its equatorial crossing point. An L-shell is a surface formed by the set of field lines that have a common L value (think of a surface of revolution of a field line around the Earth). L-shells are a useful way to characterize radiation belts because they represent trapped electron drift surfaces. The Starfish burst field line had an L value of about L = 1.12. The artificial radiation belt formed after the burst extended well beyond L = 2, with significant fluxes out to L = 4-5. The processes that might have led to formation of the broad Starfish radiation belt are still the subject of speculation to this day.

Artificial Radiation Belts *(continued)*

Both natural and artificial radiation belts pose hazards for spacecraft that operate within or through them. Energetic electrons and protons penetrate spacecraft materials creating ionization. Accumulated exposure, measured by total ionizing dose (TID), can result in damage and degraded operation of electronic components, solar cells, and mirror surfaces. The net result of TID is reduced satellite lifetimes. TID is thought to be the cause of a number of satellite failures following the Starfish test, including Telstar (launched one day after detonation), Ariel, Traac, and Transit4B. Another radiation belt hazard is differential accumulation of static charge. Subsequent electrostatic discharge (ESD) can disrupt operation or even destroy electronic devices. The charging hazard comes in two varieties: surface charging from low-energy (keV) electrons and internal or deep-dielectric charging from high-energy electrons (MeV).

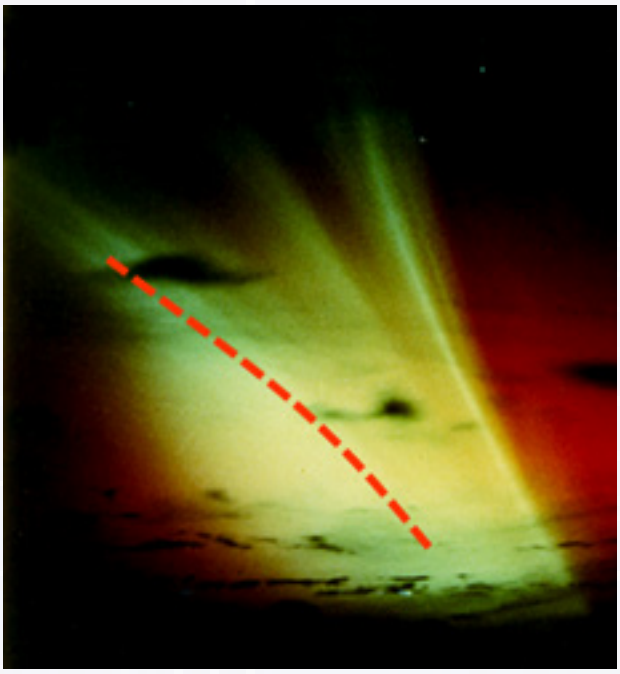

Figure 2. Photograph of disturbed environment following the Starfish test at 1 minute after burst, taken from Christmas Island. Overlaid dashed line indicates approximate location of an ambient geomagnetic field line.

Under the HANEMS (High-Altitude Nuclear Effect Modeling and Simulation Upgrades) program DTRA is funding development a first-principles model to predict artificial radiation belt environments. One of the goals of this modeling effort is to apply first-principles modeling of debris spatial distributions to the artificial radiation belt source term. High-fidelity representation of debris spatial locations translates to high-fidelity representation of artificial belt injection sites. Another goal is to investigate the consequences of the nuclear-disturbed electromagnetic environment on belt injection and evolution. In particular, how do magnetic field line distortions created by the burst alter artificial belt phenomenology? Figure 2 shows a picture of the Starfish test at 1 minute after burst. The emission evident in this picture comes from burst-generated ionization that is expanding along magnetic field lines. What is especially interesting about this picture is the upward arching of the right-most ionization filaments. For reference, the approximate location of an ambient geomagnetic field line is shown as an overlaid dashed line. At high altitudes where electrical conductivity is high, magnetic field lines are "frozen" into the background ionization. Therefore the arched filaments suggest that magnetic field lines have been similarly arched upward. Since beta electrons follow magnetic field lines, this has implications for their injection onto drift L shells.

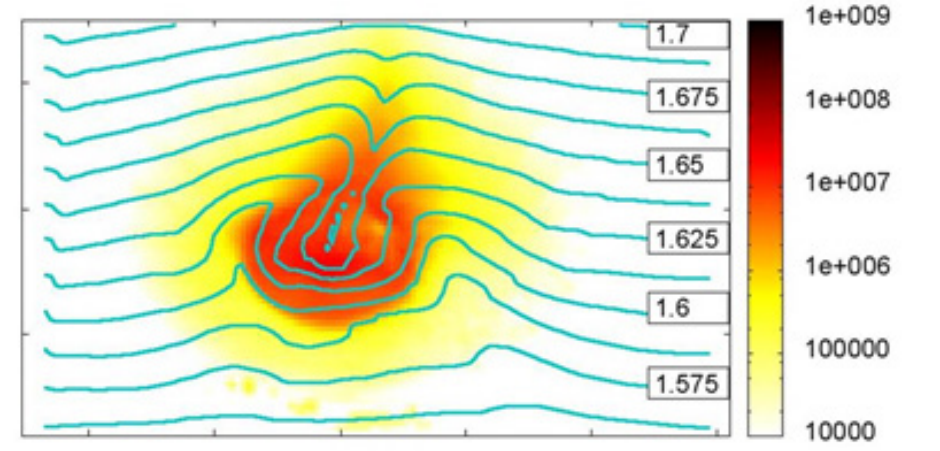

Figure 3. 2-D view of distorted L-shells (blue lines) computed from HANE first-principles simulation of several hundred kT burst at 150 km. Background color contours indicate injection source strength. Inset numbers indicate L-values.

We have captured this effect by computing trapped-particle L-shells that are distorted by a high-altitude nuclear burst. Figure 3 shows a 2-D mapping of distorted L shells at 1 minute after a several hundred kT burst at 150 km altitude. The background colors indicate beta emission source strength. In an ambient (undistorted) magnetic field

Artificial Radiation Belts *(continued)*

the L shells would be straight horizontal lines. The nature of the distortions is such that betas that would be injected onto a specific L shell in an undistorted magnetic field are injected onto a different L shell in a distorted field. This is one aspect of nuclear burst phenomenology that could play a role in broadening of artificial radiation belts.

Artificial radiation belts created by a high-altitude nuclear detonation create a hazardous environment for satellites that pass through them. Modeling the complex physical processes that govern their creation and evolution will enable high-fidelity environment prediction for assessment of system effects and mitigation strategies.

References

D. N. Baker, et al., A long-lived relativistic electron storage ring embedded in Earth's outer Van Allen Belt, Science 10.1126/science.1233518 (2013).

Dyal, P., Particle and field measurements of the Starfish diamagnetic cavity, J. Geophys. Res., 111, A12211, doi:10.1029/2006JA011827 (2006).

McIlwain, C. E., Coordinates for mapping the distribution of magnetically trapped particles, J. Geophys. Res., 66, 3681 (1961).

Mazur, J. E., An Overview of the Space Radiation Environment, Crosslink (Aerospace Corporation), Summer (2003).

Late-Time Electromagnetic Pulse

by Keith Siebert and Earl Witt (ARA)

The recognition that ionospheric disturbances have consequences for electrical systems on the ground began with the Carrington Event in 1859. While projecting telescope images of sunspots onto a screen, an amateur astronomer named Richard Carrington observed what we now know was a white light solar flare. This exceedingly large solar disturbance propagated to the Earth where it generated intense auroral displays in Earth's ionosphere. At that time the only large-scale electrical systems were telegraph lines. Telegraph operators observed current surges in their equipment to the extent that even when they disconnected the batteries powering their lines, they could still transmit messages (Kappenman, 2012).

When currents are generated in the ionosphere, they create time-dependent magnetic fields that propagate down to the ground where they can induce large-scale electric fields. These fields and associated ground surface potentials drive currents in grounded electrical systems—so-called ground induced currents (GIC). The longer the conducting network, the larger the potential drop across it, and thus the larger the magnitude of GIC. The telegraph network of Carrington's day has now been replaced by vast interconnected power grids and telecommunication lines. In power grids, transformers with grounded neutrals provide the access points for GIC. The presence of a DC current in a transformer can drive it into a non-linear regime resulting in power grid disruption through the insertion of harmonics into the grid or more seriously, transformer destruction.

High-altitude nuclear explosions also generate currents in the ionosphere. These currents can drive GIC in an analogous manner to those driven by solar activity. For the case of a nuclear explosion, the relevant electromagnetic fields are classified as E3, the third phase of high-altitude electromagnetic pulse (HEMP). It is well known that nuclear explosions create EMP. The most familiar type of EMP is the electric field pulse that is emitted nearly instantaneously after detonation. In fact there are three different phases of EMP labeled E1, E2, and E3. E1 and E2 are the nearly instantaneous emissions most commonly associated with the nuclear EMP threat. They are created respectively by gamma rays and neutrons emitted immediately after detonation. E3 is somewhat lesser known, but nevertheless just as serious a threat to technological systems. E3 is also referred to as late-time EMP or MHDEMP (where MHD stands for magnetohydrodynamic).

To refer to E3 as an electromagnetic pulse is somewhat of a misnomer. E3 is a long time-scale electromagnetic signal that can last for seconds to minutes. The mechanism by which a high-altitude nuclear explosion gener-

Late-Time Electromagnetic Pulse *(continued)*

ates E3 begins with the creation of a highly conducting ionized plasma. Magnetic field lines that thread this plasma are frozen within it, so plasma motions driven by burst energy distort field lines from their ambient locations. This creates electric currents and time-dependent magnetic fields that propagate as electromagnetic waves down to the ground. The two most important motions are radial expansion of plasma away from the burst point; and upward rise of plasma driven by coupling to upward expansion or heave of the heated neutral atmosphere. These motions further subdivide the E3 signal into two sub-categories, respectively E3A and E3B.

A key difference between naturally occurring GIC and E3 is the atmospheric environment through which the respective electromagnetic signals propagate. This is because in addition to an energetic plasma region, a high-altitude nuclear explosion creates ionization layers below the burst point that alter electromagnetic propagation. Two important layers are the x-ray patch and the beta patch. As the name indicates, the x-ray patch is created by absorption of x-rays emitted nearly instantaneously after detonation. X-ray absorption is largest in the higher density air below the burst and peak ionization generally occurs between 80 and 100 km altitude. The x-ray patch can have horizontal extents of several hundreds to thousands of km from the burst vertical. Conductivity in the x-ray patch acts to shield burst-generated electromagnetic signals from the ground below. These signals must either diffract around the edges of the x-ray patch or diffuse through it, thus altering both the magnitude and timing of the ground signal. The beta patch is a much more horizontally-localized ionization region below the burst point. It is created by electrons from beta decay of fission products. These electrons follow magnetic field lines down toward lower-altitude air where they are absorbed. Ionization from beta absorption is generally peaked around 60–70 km. Complicating matters further is the fact that conductivity within x-ray and beta patches is anisotropic, having both Pedersen (diagonal) and Hall (off-diagonal) components. Patch conductivity is also time-dependent, decaying due to recombination chemistry.

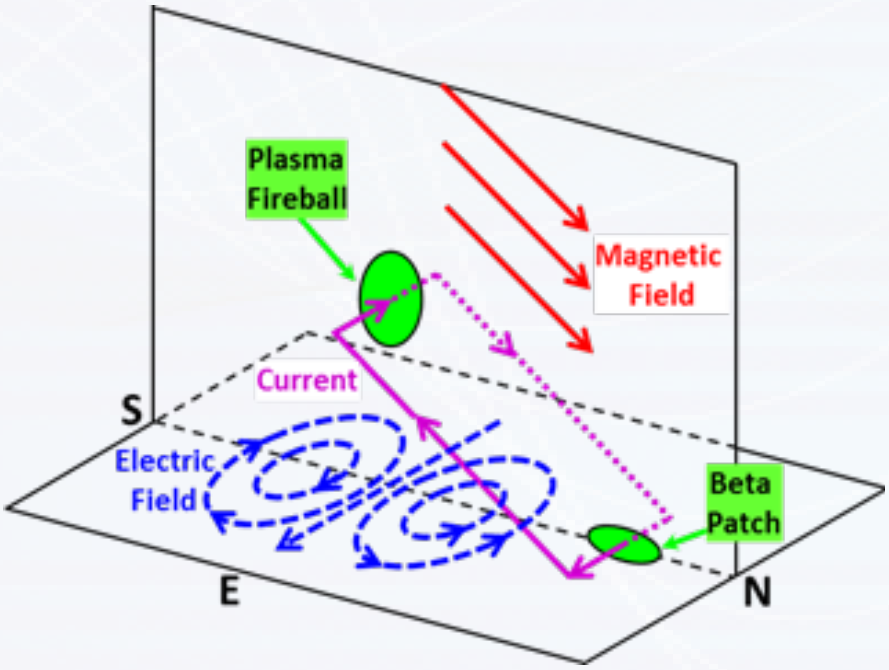

Figure 1. Schematic of heave current circuit showing directions of ambient magnetic field (red), electric currents (purple) and ground electric fields (blue). In this circuit the plasma fireball acts as the generator and the beta patch acts as the load.

The beta patch plays a key role in E3B phenomenology. E3 researchers have long recognized that the beta patch is one element of a heave current circuit that drives E3B. This circuit is schematically illustrated in Figure 1. Rising plasma in the burst-created fireball acts as a dynamo, and beta patch ionization acts as a load. These two elements are connected by currents (purple lines in the figure) that flow parallel to magnetic field lines (red) on the east and west sides of the fireball. Arrowed blue curves show the ground electric field pattern associated with this simplified current circuit. Note that the ground electric field has a two-cell pattern oriented such that the electric field is predominantly directed towards the east below the burst. This general pattern and orientation is consistent with E3B predictions from the HEMPTAPS code, DTRA's legacy EMP model (Gilbert, et al. 2010).

Modeling E3 is challenging because of the interplay of myriad physical processes. To address this, DTRA recently funded the development of a first-principles E3 model. The "E3 Model" was constructed by coupling a

Late-Time Electromagnetic Pulse *(continued)*

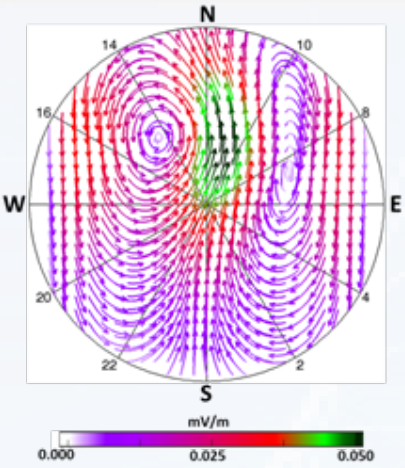

Figure 2. Ground electric field pattern computed from E3 Model for a low-latitude burst over ocean. View is from above and centered on the burst vertical.

first-principles HANE model with an electromagnetic solver. The HANE model computes burst-generated currents and electromagnetic fields in the ionosphere, and the EM solver propagates these fields down to and into the ground. With the E3 Model we were able to discover a previously unanticipated aspect of E3 phenomenology. Figure 2 shows the ground electric field pattern from a low latitude burst simulation using the E3 Model. The pattern has the same two-cell morphology as predicted by the simple circuit model, but the orientation of the pattern is rotated 90 degrees counterclockwise when viewed from above. Thus instead of being eastward, the predominant electric field pattern below the burst is directed northward. Analysis of this and other simulations reveals that the cause of the rotation is Hall conductivity in the beta patch. Hall conductivity acts to tilt the current circuit around the central axis connecting fireball and beta patch. We have corroborated the northward directed electric field against data. This prediction has important consequences for coupling of E3 fields to long-line power grids as the relative orientation of ground fields and power grids determines coupling effectiveness.

E3 is a significant HANE threat. Models such as the E3 Model give DTRA a tool for high-fidelity E3 prediction, and reveal previously unknown phenomenology. The similarity between naturally occurring GIC and E3 presents further opportunities for E3 model validation as well as leveraging new GIC data for integration within E3 models.

References

Kappenman, J., A perfect storm of planetary proportions, IEEE Spectrum, February (2012).

Gilbert, et al., The late-time (E3) high-altitude electromagnetic pulse (HEMP) and its impact on the U.S. power grid, Metatech Report, Meta-R-321 (2010).

Space Weather Opportunities for HANE Model Validation

by Keith Siebert (ARA)

One of the most difficult aspects of HANE model development is the dearth of nuclear test data for code validation. HANE phenomenology is strongly dependent on burst-altitude, and within each burst altitude regime there are at most one or two relevant tests. In some regimes, for example, the very high altitude regime (burst altitudes greater than approximately 600 km), there is no test data at all. Furthermore the tests were conducted in the late 1950s and early 1960s when instrumentation was not as sophisticated as it is today. HANE phenomena have several analogs to naturally occurring phenomena in the space environment. In this article we consider each of these analogs in greater detail, and discuss how we can use space environment data and models to improve and validate DTRA's HANE models.

One such space environment modeling tool is DTRA's Integrated Space Weather Prediction Model (ISM). ISM is a first-principles, 3-D, time-dependent, magnetohydrodynamic (MHD) model of the near-Earth and distant space environment. ISM's computational volume extends from below Earth's ionosphere out into the magnetosphere and solar wind. ISM simulations are driven by solar wind boundary conditions specified on the sunward boundary of its grid. Figure 1 shows pressure contours from an ISM simulation, and illustrates the scale of the computational volume. In this graphic the solar wind is coming in from the right hand side. Its impact on the Earth's magnetic field creates a shock upstream from the Earth (the bow shock), and stretches out magnetic field lines on the downstream side creating the magnetotail. The diagonal light-blue structure in the upstream

Space Weather Opportunities for HANE Model Validation *(continued)*

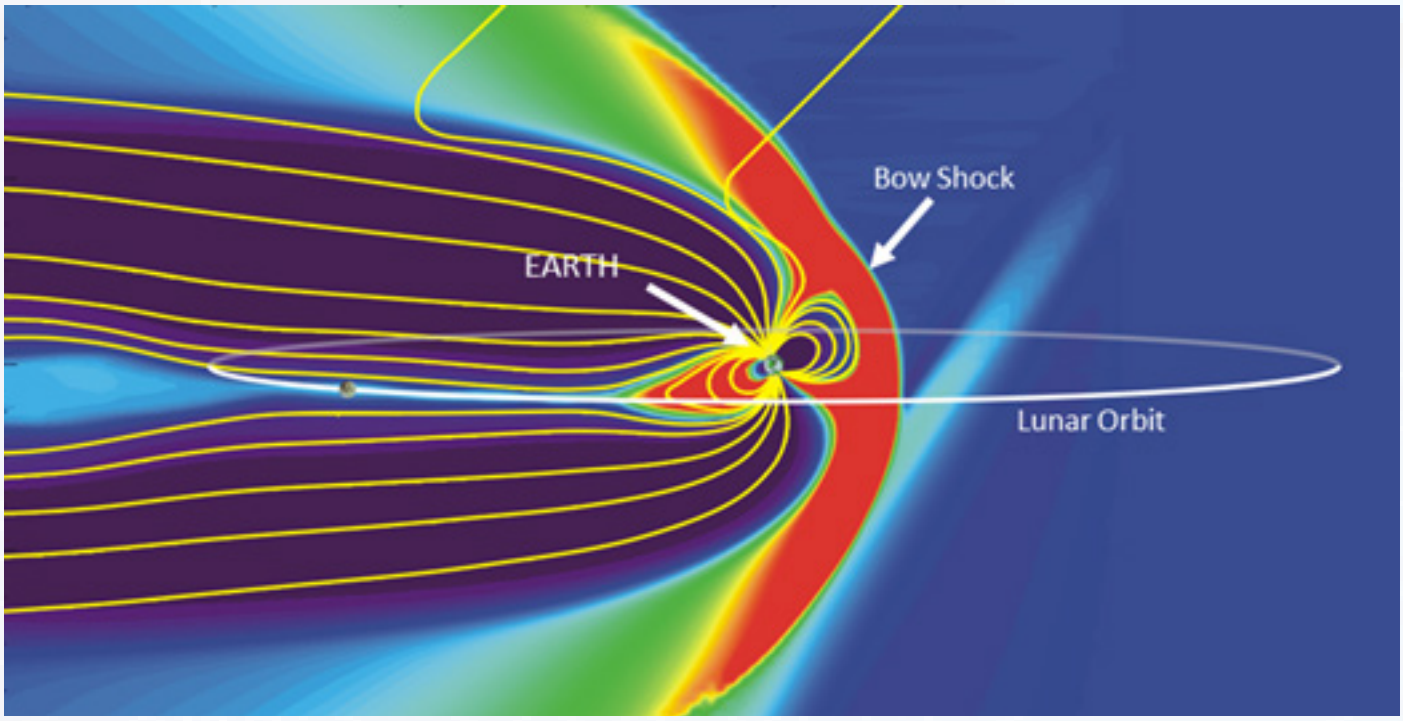

Figure 1. Pressure contours and magnetic field lines (yellow) from an ISM simulation. Solar wind is directed from right to left.

solar wind region is a discontinuity that has just become incident on the bow shock. ISM is based on the same MHD model and numerical algorithms as DTRA's first principles HANE model, Multi-Fluid MEGS.

ISM has particular application to code validation for E3 modeling. As discussed previously E3 is analogous to naturally occurring GIC driven by solar activity. The E3 Model (discussed in the Late-Time EMP article) was constructed by coupling the HANE model, Multi Fluid MEGS, with an electromagnetic (EM) solver. Since the EM Solver was designed to be modular, it can be coupled to any MHD model. Thus by driving the EM Solver with ISM instead of Multi-Fluid MEGS, we can derive a capability for GIC modeling. In this mode, ISM computes the ionospheric current systems that are ultimately driven by solar activity, and the EM Solver propagates the attendant electromagnetic fields down to and into the ground. Comparison of model predictions with GIC data collected for specific solar events then provides an additional means for E3 Model code validation.

Validation of artificial radiation belt models using space data takes advantage of the observation that once formed, an artificial radiation belt is subject to the same physics that governs evolution of the natural belts. So by substituting a nuclear injection with a naturally occurring injection we can compare the subsequent evolution and decay predicted by the model with satellite data. The recently launched Van Allen Probes are ideal for this kind of code validation. In addition to providing detailed data about the dynamics of radiation belt particle fluxes, the Van Allen Probes are also instrumented to measure properties of electromagnetic waves in the belts (Mauk, et al. 2012). Low-frequency electromagnetic waves (VLF and lower) are able to interact with radiation belt particles and change their orbits so that they penetrate deeper into the atmosphere where they can be absorbed. This particle scattering process plays in important role in the long-term decay of injected belts. It is typically modeled as a diffusion process in velocity space. Data collected from the Van Allen Probes will aid in establishing better models for diffusion coefficients, including dependence on space environment conditions.

The instability mechanisms that structure ionization plumes following a high-altitude nuclear detonation are similar to those that operate in equatorial regions of Earth's ionosphere. Structuring of the equatorial ionosphere is referred to as Equatorial Spread F (ESF). Whereas in the nuclear case it is a plasma density

Space Weather Opportunities for HANE Model Validation *(continued)*

enhancement (the nuclear plume) that breaks up into smaller-scale irregularities, in the naturally occurring case it is rising plasma depletions or "bubbles" that break up. Nevertheless, the statistical models developed for evolving nuclear structure should be applicable to the natural environment as well, and thus might allow for further code validation. In addition, data collected from ESF measurements might shed light on the spectral distribution of irregularity scale sizes that underlies the statistical models. Under the HANEMS Program, Northwest Research Associates has undertaken an analysis of data collected from the Communications/Navigation Outage Forecasting System (C/NOFS) experiment to improve HANE spectral distribution models.

This brief survey of space environment phenomena with analogs to HANE phenomena is not exhaustive, but rather provides an introduction to how we might use space data and models to improve and validate HANE models. Space weather research is an active field both in terms of data collection and modeling, and provides many opportunities for cross-fertilization with HANE modeling efforts.

Reference

B. H. Mauk et al., Science objectives and rationale for the Radiation Belt Storm Probes mission. Space Sci. Rev. 10.1007/s11214-012-9908-y (2012).

Maintaining and Protecting Your Social Media Fingerprint

Some people love social media almost to the point of narcissism, and some people refuse to use it and decry the lack of real-life interaction that comes from it. Social media is a way to share the sublime—the lofty, grand, or exalted in thought, expression, or manner—but it can also be used to share the innately mundane aspects of life. It is both a pleasure and also a pain. While we awant some people to have our data, we also don't want others rooting around our most personal, and sometimes awkward, moments. However, social is not going away anytime soon.

In the era of social media, a social media fingerprint is almost as important as your credit score. Creating and maintaining your social media fingerpring is important for many reasons: (1) to ensure no one else is creating a profile and pretending to be you, (2) to keep an online fingerprint that accurately represents you, and (3) to monitor what is being placed on your online fingerprint from malicious actors.

What is Social Media and Why Might It Matter?

Social media (Facebook, Twitter, Instagram, Vine, and LinkedIn, among others) is a way to communicate with people instantly anywhere around the world. Social media is seen as a potential threat in many areas of the world; for example, social media was used in organizing the Arab Spring movement. While we embrace it, governments and other areas in the world moniter social media as seen as a cause for social unrest, rather than the outlet of some much more deeper cultural and societal issues.

Social media is used by collection agencies, government, commercial entities for employment, and credit companies. Forbes in a tech article states that social media can even be used as another method for social science: "Facebook is an ideal environment for studying human behavior. Every click, like, friend acceptance (or rejection), and peek at an ex's profile is tracked for millions of people every day" (Hill, 2013).

A different Forbes article discusses the potential of your social media profile to affect your employment status. According to the article Microsoft Research stated that in 2010, 70% of recruiters said they would reject applicants based on information they found online—or what they did not find: "The most frequent sin committed by the erstwhile job seekers was not drinking (reason for the rejection 9% of the time) or drugs (10%) or having a mutual Facebook friend that the employer thinks is a total skeezeball (0%), but getting caught for lying about their qualifications (13%)" (Hill, 2011). It is now common practice to search job candidates on the internet, and a carefully maintained social media profile will allow you to leave a good impression.

Maintaining and Protecting Your Social Media Fingerprint *(continued)*

Apps, Links, and Contacts

You may not know it, but many applications (apps) on social media are not your friend. The apps say they are free, but they may require access to your friend lists and other personal information. Do you really want a third-party application built by who-knows-whom to access to your pictures, friends, family, phone numbers, email addresses, and other information? Be cautious of what applications you accept. There have been many reports of apps that are full of vulnerabilities, opening up ports on your computer to malicious code that collects information on what you do, when you do it, and for how long. DISA's social media training states these programs can trick users into giving up credit card or login information. Any app that needs your username and password is not to be trusted. Any app that asks for your username and password to "generate a list of your contacts" is not, I repeat, not to be trusted! Don't give these apps more power than they already have and don't give them more access than they need. NEVER give out your user name and password—no matter how many times the site says "don't worry—you can trust us."

Additionally, never click on a link that you are unsure of or that is a shortened link that hides the real address (tiny URLs). Some viruses and worms send themselves automatically, so you could get one in a seemingly trusted message from a friend. Even advertisements can hide malware. DISA recommends never opening any software though a social networking service. Aways open it from the software's official website.

Do no to let Facebook access your contacts. Yes, it is interesting to see who is proposed to be your friend, but not only does Facebook upload your contacts, it also downloads everyone it thinks should be your contact to your phone. You will soon see your contact list on your phone fill up with hundreds of miscellaneous emails, phone numbers, and minutia. After realizing what Facebook (and other social media apps like Google+) was doing, I spent a day or so sifting through the hundreds of contacts that were downloaded to my smart phone—including an email contact that my wife set up for our cat (she needed another "friend" to get more Farmville points)! Unless you want to spend quality time sifting through your contact list and deleting whatever that is downloaded to your phone, don't let these apps have access to your contacts.

Now I'm Terrified!

While we both love and hate social media, it is here for good. One needs to be aware of several cautions. DISA details the perils of social media in their unclassified social medial training found at http://iase.disa.mil/eta. The training reviews how social media can be a great way to keep in touch with people even when you are far away, but remember that just because someone friended you, does not mean they are actually your friend. It also reiterates that providing too much information leave vunerabilityes for people to hack your online accounts, steal your identity, steal from you, or do physical harm.

Do This, Not That

Don't share information that you do not want to become public. If you post your work on social media, you can be targeted because you have connections to DOD. Even listing hobbies, groups, or likes can reveal information about you that can compromise your safety, not to mention your job! It may be a good practice to disable the GPS tracker on your cell phone. Never talk about things like passwords, locations (especially while on vacation and no one is home—you are a perfect target for a home robbery!), or anything sensitive like your birthday or any political, defamatory, obscene, abusive, racist, bullying, or otherwise offensive or illegal information—and please remove that 1977 picture of you and your friend Barry. Instead, keep things light, limit who can see your profile, be wary of strangers, and, most of all, be sure to stay honest. These days, every keystroke counts.

References

Hill, Kashmir. 46 Things We've Learned from Facebook Studies. *Forbes.com.* 21 June 2013.

Hill, Kashmir. What Prospective Employers Hope to See in Your Facebook Account: Creativity, Well-Roundness, and 'Chastity'. *Forbes.com.* 3 October 2011.

DTRIAC Collection Additions

DTRA Technical Reports

DTRA-TR-12-04, Radiation Internal Monitoring by In Vivo Scanning in Operation Tomodachi

Radioactive materials were released into the environment following the accident at the Fukushima Daiichi Nuclear Power Station following the earthquake and tsunami in Japan on March 11, 2011. Individuals in Japan affiliated with the DOD were exposed to these materials during Operation Tomodachi, and in response the DOD conducted the internal monitoring (IM) program described in this report, More than 7,900 DOD-affiliated individuals were internally monitored as part of this program from 16 March to 31 August 2011, at both CONUS and OCONUS locations. About 3% of those monitored had a measured activity greater than the minimum detectable activity (MDA). Those persons with measured activities greater than MDA had a maximum committed effective dose of 0.25 mSv (0.025 rem) and a maximum thyroid committed equivalent dose of 4.2 mSv (0.42 rem). In addition to descriptions of IM equipment, procedures, methodologies, and monitoring results, the report also includes discussions of the IM program's concept of operations, radiation safety directives, and quality assurance program.

DTRA-TR-12-41, Radiation Dose Assessments for Fleet-Based Individuals in Operation Tomodachi

This report provides the radiation dose assessments for the DOD fleet-based population of interest that was potentially exposed to radioactive fallout resulting from the Fukushima Daiichi nuclear power station units' radiological releases that followed the earthquake and tsunami on March 11, 2011, The associated DOD disaster relief operation to the citizens of Japan was entitled Operation Tomodachi. Finalized radiation dose assessments for the population of interest should be loaded into an Operation Tomodachi Registry by the end of 2013, which will support public inquiries.

DTRA-TR13-59, Fast GC-MS for Analysis of CW Materials

This final report documents the continuation of the Constellation Technology Corporation's (Constellation's) work for DTRA on new analytical techniques for chemical weapons (CW) material. The previous task, Task 24.1, investigated a commercially available fast gas chromatography (GC) equipped with a pulsed-flame photometric detector (PFPD) for fast separation and detection of CW degradation compounds containing sulfur, phosphorus, and nitrogen. Because of the success of Task 24.1 as a proof of concept, Constellation was directed to pursue further investigation in fast gas chromatography. The purpose of this task, Task 24.2, was to evaluate the feasibility of performing fast separation, detection, and identification of CW degradation compounds using the same fast GC equipped with a mass spectrometer (MS) detector. An MS detector allows for simultaneous detection and identification of virtually any compound that is eluted from the GC.

DTRA-TR-13-61, Photodetector

This report describes the extension of photodetector technology to large devices capable of close-pack operation, the equipment and methods developed, and the experimental data evaluating the device performance.

DTRA-TR-13-62, Chirped Grating Tunable Lasers for the Infrared Molecular Fingerprint Spectral Region

A new approach approach to tunable mid-infrared lasers, an optically pumped, type-II, InGaSbllnAs gain medium with a chirped distributed feedback grating, has been developed. The chirped grating is patterned using an interferometric lithography (IL) technique with spherical wave fronts and etched into the top cladding of the laser slab waveguide structure. A reduced longitudinal chirp grating fabrication technique has been developed that dramatically extends the single frequency tuning range. Continuous tuning of 80 nm around 3.1 μm with 320 mW single facet output power at 80 K and a 1.6-nm FWHM is reported. The present device is designed in the 3- to 4-μm range, which matches a low loss atmospheric transmission window, and covers an important region of molecular vibration spectra, in particular, the hydrocarbon C-H stretch at 3.3 μm, making it suitable for atmospheric pressure remote gas sensing of industrially important small molecules such as methane, hydrogen chloride and ammonia.

DTRA-TR-13-63, Growth and Characterization of Nanostructured Glass Ceramic Scintillators for Miniature High-Energy Radiation Sensors

Synthesis and characterization of scintillation crystals was performed at the Los Alamos National Laboratory (LANL). Melt quenching and sol-gel synthesis were applied to prepare various glass ceramic scintillators. For the first time ever, a glass ceramic containing 35 mol% LaF3:Ce3+ was made. Differential scanning calorimetry, x-ray diffraction, transmission electron microscopy, nuclear magnetic resonance, photoluminescence and radioluminescence spectroscopy, and FTIR/Raman spectroscopy and neutron scattering measurements were performed. Temporal dynamics was investigated by ultra-short bursts of XUV radiation at UNM. The rise time was resolved using Kerr gating technique with 8 ps resolution. Spectro-tem-

DTRIAC Collection Additions *(continued)*

poral dynamics was resolved using streak camera and tunable pump at second/third harmonic (400/267 nm) and XUV. Observed rise time scaling is consistent with chromophore trap dynamics. Rise time of approximately 80 ps in glass ceramics was measured for the first time. Varying plasma parameters as well as excitation pulse characteristics optimized XUV generation efficiency by 40 times compared to standard yield. Combined with improved collection efficiency, newly developed UNM scintillation dynamics lab is now ready for characterization of various scintillators for future material optimization.

DTRA-TR-13-64, Nanowires for THz Spectroscopy

Detailed experimental investigation of THz emission mechanisms in InAs nanowires is performed. Multiple independent measurements are brought into quantitative agreement by means of the developed model, which includes contributions of quantized surface plasmon modes of the cylindrical nanowire geometry. THz emission from ordered array of InAs nanowires is also investigated, and model predictions are verified using developed broadband THz spectrometer. Novel pyramid hexagonal lattice structures developed during this work have proven as extremely broadband (octave-spanning) THz nanoscale emitter sources with attractive potential for a variety of applications. To perform broadband measurements, novel THz spectrometer has been developed with operating up to 20 THz. Novel electro-absorption sampling technique has been developed using multiple quantum well structures. Franz-Keldysh effect has been identified as the main detection mechanism and coherent detection of THz pulses has been demonstrated. THz imaging with electro-absorption effect using conventional (visible wavelengths) imaging systems has also been demonstrated.

DTRA-TR-13-65, LPOSS Miniaturization and Method Development

Further miniaturization of the sequential injection based instrument development under a previous contract was accomplished. The instrument is targeted at the determination of chemical weapons (CW) compounds, such as precursor and degradation compounds. The primary classes of CW agents being targeted are those derived from phosphoric acid. In addition to reducing the size and weight of the current instrument, a feasibility study was performed to evaluate reducing the size and weight to that which may be hand-held. Development of a methodology that reduced the time of analysis and lowered the detection limit of these compounds was performed. Other mechanisms were investigated, including hydrolysis and enzymes assisted degradation, for breakdown of the chemical species to be determined. An investigation of mechanisms to extend the half-life of the chemical agents was also performed.

DTRA-TR-13-66, Thin Film Mercuric Iodide

Large area x-ray imaging has wide application in the medical and industrial fields. Currently, the material of choice is amorphous selenium. Mercuric iodine offers many advantages over selenium in a thick film, larger area application, such as x-ray hardness, greater sensitivity, and scaling. Polycrystalline mercuric iodide coated on amorphous silicon flat panel thin film transistor arrays are the best candidate for direct digital x-ray detectors for radiographic and fluoroscopic applications in security applications and medical imaging based upon atomic number, energy band gap and charger pair formation energy. A number of companies have been exploring the use of mercuric iodide as an alternate semi-conductor coating for medical imaging as well as security issues, such as cargo inspection.

DTRA-TR-13-67, Standardized Unclassified Little Boy and Fat Man Outputs

This report provides detailed neutron and gamma output information for the Fat Man and Little Boy devices. It has been prepared for DTRA for use by the agency, its contractors, and other interested parties in analysis of environments and effects generated by low-technology, fission-only nuclear devices. The detailed spectra given here are the same as those published previously by White and coworkers. This report has different goals than the earlier reports, and the results presented are limited to those useful for the prediction of weapons-generated environments. Specifically, we have restricted the presentation to prompt neutron and gamma outputs.

DTRA-TR-13-68, 2013 Technology Readiness Evaluation of Defense Threat Reduction Agency Basic Research 6.1 Active Grants FY-08 through FY-12

The DTRA Basic Research Program employs Technology Readiness Evaluations (TREs) annually for the assignment of Technology Readiness Levels (TRLs) to basic research projects funded as part of the Basic Research portfolio. The TRE process informs the Basic and Applied Sciences leadership on the overall maturity of its basic research (6.1) program, the readiness of certain basic research projects to transition to applied research (6.2), and the appropriateness of certain projects for extending the 6.1 funding.

DTRIAC Collection Additions *(continued)*

DTRA-TR-13-69, Nuclear, Biological, Chemical (NBC) Instrument

Constellation Technology Corporation (Constellation) has designed a fourth configuration of the NBC instrument in a multi-year spiral development that has most recently seen the merging of additional capability, some miniaturization of subsystems, adaptation to different application platforms, and an optimization of the overall control and reporting software. The latest NBC is an integrated platform with complete algorithm coverage of a long list of threats in the three categories of interest. It includes an air sampler, which supplies the biological and chemical detectors with ambient material in a user-defined CONOPS. It is a man-portable backpack and can facilitate directed air sampling by a flexible inlet hose. This mode of directed sampling could be advantageous with suspected explosive compounds.

DTRA SMALL BUSINESS INNOVATION RESEARCH

SBIR 2982-DTRA-IS, Toughened Fabrics with Counter-WMD Functionality for Daily Wear

Military personnel and first responders must be prepared to operate under a wide range of CBRNE threats (chemical, biological, radiological, nuclear, high explosive) and rapidly counter WMD hazards. Daily-wear uniforms such as the army combat uniform (ACU) or the CWU-27/P flight suit are breathable and lightweight, providing basic abrasion and fire protection, but are not capable of significant CBRNE protection. On the other end of the spectrum, CBRNE suits offer protection from a variety of WMD threats, but must be donned post-WMD-event because they are heavy, easily punctured or torn, and exhibit poor breathability and launderability. This lack of multifunctional garments for soldier protection significantly degrades survivability. New materials are sought to significantly enhance the counter-WMD/CBRNE functionality of the ACU or CWU-27/P while remaining lightweight, breathable, and durable. Luna, teaming with a major U.S. uniform manufacturer, developed a method to reliably fabricate large-scale quantities of modified nylon/cotton (NYCO) fabric.

TECHNICAL NOTE

DTRA TN-I 2-004, Cratering Critical Depth

The Defense Nuclear Agency sponsored a Critical Depth of Burial (CDOB) Program in 1989 that focused on the SULKY event (an 92-ton nuclear detonation in dry basalt below Buckboard Mesa, Nevada Test Site, on 18 December 1964). The only report the CDOB Program produced was a joint summary paper entitled DNA CDOB Program and the SULKY Retarc Status Report. This technical report focuses on the SULKY findings (field and lab data, calculations, and centrifuge modeling) from both the original studies in the 1960s and their reanalyses during the CDOB Program. Although SULKY was predicted to produce an ejecta crater based on high-explosives prediction data, current nuclear prediction data suggests it was buried too deep to produce an ejecta crater. The SULKY mound (retarc) consisted of about 4 ft of rubble overlying a series of fault blocks consisting of jointed basalt with fault planes that dipped inward to a location below surface ground zero (SGZ). The fault blocks had small offsets to their adjacent blocks. The jointed basalt within the fault blocks was relatively undisturbed. The central depression on the SULKY mound was mostly a spall crater with a depth of at least 4–7 ft and a radius of about 35–40 ft. The hinges of overturned flaps occurred near the edges of the SULKY spall crater at ranges of 44 ft and 50 ft from SGZ. A very small amount of venting occurred during the SULKY event. The CDOB scaled centrifuge tests in simulated rock produced fault block displacements and spall analogous to that for SULKY. The CDOB 2-D finite-difference calculations produced a surface velocity profile in agreement with the high-speed photographic data. Those calculations also predicted the SULKY cavity radius fairly well. However, the calculations predicted spall from the preshot ground surface to the top of the cavity. The data do not support this. Thus, the subsequent CDOB discrete element calculations that used the finite-difference velocity profiles as initial inputs did not predict a retarc.

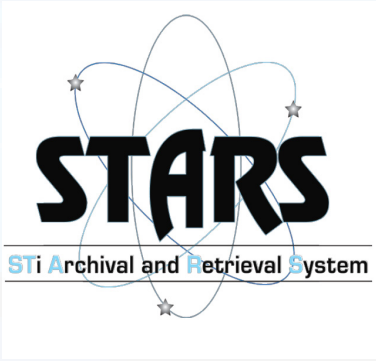

Ask the IAC

What kind of support does DTRIAC have available at the DTRC?

The Defense Threat Reduction Center (DTRC) at Ft. Belvoir, Virginia, houses the DTRIAC Scientific and Technical Information (STI) Support Center. The STI Support Center staff is able to support your projects in a variety of ways, including conducting research, obtaining reports, and providing editorial assistance.

The STI Support Center has DTRIAC librarians who are ready to assist with any research question or literature search. DTRIAC librarians are a direct link to DTRIAC resources as well as DTRA subject matter experts. They also have experience searching the STI Archival and Retrieval System (STARS), Defense Threat Information Center (DTIC) database, and other databases to help you retrieve any scientific or technical literature or media material.

Additionally, the STI Support Center has a technical editing staff ready to help ensure proper formatting, submission, and archival of your reports, allowing them to be widely disseminated through both DTRIAC and DTIC.

Please contact the DTRIAC STI Support Center for any assistance via email (dtriac@dtra.mil), phone (703-767-5892), or in person (HQ DTRC, Room 3880).

This Quarter in History

October 31, 1952 — IVY MIKE, the first full-scale thermonuclear device, was detonated in a test at Eniwetok in the Marshall Islands. Due to its weight, the weapon design was not deployable.

October 31, 1958 — A voluntary moratorium on nuclear testing began. The moratorium officially ended in 1959, but no testing occurred for 34 months. The hiatus in testing ended on 1 September 1961 when the USSR once again began atmospheric tests.

December 10, 1935 — Professor James Chadwick was awarded the 1935 Nobel Prize in Physics for proving the existence of the neutron. The addition of the neutron to the model of the atom allowed physicists calculate the binding energy of nuclei and to produce heavy atoms, such as uranium.

December 19, 1950 — The first edition of *The Effects of Atomic Weapons,* edited by Dr. Samuel Glasstone, is published. It was later retitled *The Effects of Nuclear Weapons*. This publication is still available for distribution from DTRIAC.

December 1958 — The Defense Reorganization Act places the AFSWP under the control of the Joint Chiefs of Staff (JCS) and renamed the Defense Atomic Support Agency (DASA).